Various Directional Wave Spectra Obtained from a GNSS Buoy

Yen-Pin Lin* Ching-Jer Huang** Sheng-Hsueh Chen*** Chia Chuen Kao****
* Coastal Ocean Monitoring Center, National Cheng Kung University, Tainan.
Email: lyb57@mail.ncku.edu.tw
** Coastal Ocean Monitoring Center, National Cheng Kung University, Tainan.
Email: cjhuang@mail.ncku.edu.tw
*** Coastal Ocean Monitoring Center, National Cheng Kung University, Tainan.
Email: sean284@mail.ncku.edu.tw
**** Coastal Ocean Monitoring Center, National Cheng Kung University, Tainan.
Email: kaoshih@mail.ncku.edu.tw

Abstract

Lin et al. (2017) developed a Global Navigation Satellite System (GNSS) buoy for monitoring water surface elevations in estuaries and coastal areas. The directional wave spectrum was obtained from analyzing the altitude, and the velocities in the east and north directions. This study aims to determine the directional wave spectrum by utilizing various combinations of the GNSS buoy data, such as the displacement in the east, north, and upward directions (enη) and the velocities in the east, north, and upward directions (uvw). The three combinations are ηuv, enη, and uvw. We find that the mean direction at the peak frequency, the directional spreading at the peak frequency, and the dominant (peak) wave direction obtained by utilizing these three combinations are almost identical. Besides, the mean direction at the peak frequency and the dominant wave direction are nearly identical. Furthermore, the directional wave spectra are very similar by utilizing three combinations, especially when the significant wave heights are larger than 1 m.

Keywords: GNSS buoy, Dominant wave direction, Mean direction, Directional spreading

I. Introduction

Ocean wave heights, periods, directions, and tide data are very important to coastal engineering and coastal protection, e.g., the determination of the run-up height on the seawall needs tide and wave data simultaneously.

Based on the Virtual Base Station Real-Time Kinematics (VBS-RTK) positioning technology, Lin et al. [1] developed a Global Navigation Satellite System (GNSS) buoy for monitoring tides and ocean waves simultaneously in estuaries and coastal areas. The tide levels obtained from the GNSS buoy were consistent with those from a neighboring tide station. The root-mean-square error of the tide data was within 10 cm. The water surface elevations, significant wave heights, zero-crossing periods, one-dimensional wave spectra, directional wave spectra, and dominant (peak) wave directions derived from the GNSS buoy were consistent with those obtained from the accelerometer-tilt-compass (ATC) sensor. The GNSS receiver obtained time-series data of six parameters, including the longitude, latitude, altitude, and the velocities in the east, north, and upward directions. Lin et al. [1] utilized only the water surface elevation and the velocities in the east and north directions (henceforth ηuv) to obtain the directional wave spectrum and directional wave parameters. Riedel and Healey [2] indicated that by combining time-series data of various parameters , such as the displacement in the east, north, and upward directions (henceforth enη) and the velocities in the east, north, and upward directions (henceforth uvw), the directional wave spectrum and its spectral parameters could also be calculated.

Work [3] compared wave data obtained from a data buoy with those from an acoustic Doppler current profiler (ADCP). He utilized the maximum entropy method (MEM) to analyze the directional wave spectrum of both systems. For the data buoy, time-series data of three linear and three angular motions were used. For the ADCP, time-series data of twelve velocities were utilized. The twelve velocities are composed of velocities at the upper three layers with each layer has four-beam velocities. He found that the wave energy of the ADCP was more tightly concentrated around the predominant direction and indicated this was due to that the six time series from the data buoy were measured at a point; however, twelve time series from the ADCP were measured at three layers near the top of the water column. That was to say, combination of different parameters might lead to differences in directional characteristics.

This study aims to investigate the differences in the directional wave spectrum and directional wave parameters obtained by utilizing various combinations of the time-series data of enη and uvw

from the GNSS buoy. These combinations include ηuv, enη, and uvw.

II. Methodology

The working principle of the GNSS buoy and the GNSS accuracy specifications had been presented in Lin et al. [1]. The deployment of the Small Liu-qiu buoy and the data acquisition were presented at Section 4.1.2. in Lin [4]. Inclination data are not utilized in this study to correct water surface elevations. The field data were collected from 00:00 October 15 to 23:00 October 30, 2016. Hourly data whose percentage of good altitude data equals to 1.00 are utilized. The maximum significant wave height was near 7 m. The definition of the percentage of good altitude data is shown as follows. The outlook and location of Small Liu-qiu buoy are shown in Figs. 1 and 2, respectively. In this study, the water surface elevation, the displacement in the east and north directions, the velocity in the east, north and upward directions are denoted by η, e, n, u, v, and w, respectively.

A. Percentage of good altitude data

According to factors, including the signal received by the GNSS buoy and the GNSS base station network, the network signal quality of the GNSS buoy and the GNSS base station network, and the ionospheric activity, the GNSS buoy obtains specific resolution results with specific quality indicators. When the quality indicator shows "4 – RTK Fix solution," the instantaneous resolution result is identified as good altitude data. Thus, the hourly percentage of good altitude data, PGAD, is determined as the ratio of the number of good altitude data, GAD, to the number of observed data (512), and defined as follows.

$$PGAD = \frac{GAD}{512} \tag{1}$$

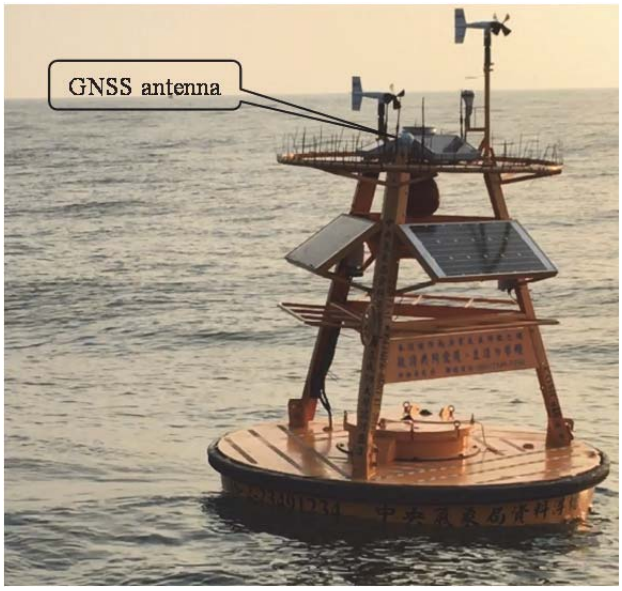

Figure 1. The outlook of Small Liu-qiu buoy

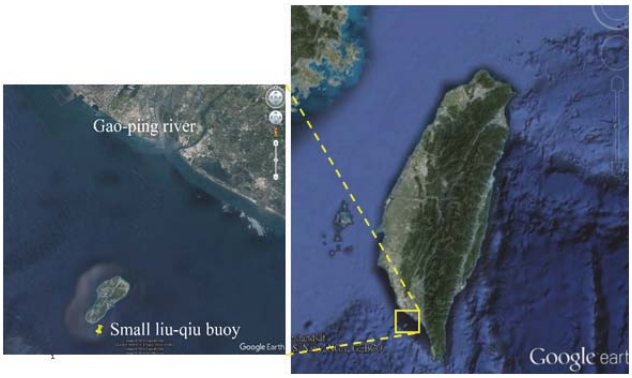

Figure 2. The location of Small Liu-qiu buoy

B. Directional wave spectra obtained from ηuv data

According to Lin et al. [1], the directional wave spectrum, $S(f,\theta)$, can be determined as follows.

$$S(f,\theta) = D(f,\theta)C_{\eta\eta}(f) \tag{2}$$

$$D(f,\theta) = \frac{1}{\pi}\{\frac{1}{2} + \sum_{n=1}^{2}[a_n'(f)\cos n\theta + b_n'(f)\sin n\theta]\} \tag{3}$$

where *f* is the frequency, θ is the wave propagation angle measured from the x-axis and increases in the counterclockwise direction, $D(f,\theta)$ is the directional spreading function, $C_{\eta\eta}(f)$ is the one-dimensional spectrum, $a_n'(f)$, $b_n'(f)$ are the Fourier coefficients, and *n* is the order of the Fourier series.

Lin et al. [4] transformed time-series data of the altitude obtained from the GNSS receiver into those of the water surface elevation. We also derived the equations for the Fourier coefficients of the directional spreading function using the GNSS time-series combination of ηuv . Hence, the one-dimensional spectra, significant wave heights, zero-crossing periods, peak periods, directional wave spectra, and dominant wave directions were obtained. The Fourier coefficients of the directional spreading function were determined as Equations (4) – (7).

$$a_1'(f) = \frac{C_{\eta u}(f)}{\sqrt{C_{\eta\eta}(f)[C_{uu}(f)+C_{vv}(f)]}} \tag{4}$$

$$b_1'(f) = \frac{C_{\eta v}(f)}{\sqrt{C_{\eta\eta}(f)[C_{uu}(f)+C_{vv}(f)]}} \tag{5}$$

$$a_2'(f) = \frac{C_{uu}(f)-C_{vv}(f)}{C_{uu}(f)+C_{vv}(f)} \tag{6}$$

$$b_2'(f) = \frac{2C_{uv}(f)}{C_{uu}(f)+C_{vv}(f)} \tag{7}$$

where $C_{mn}(f)$ was the cross-power spectrum between the m-th and n-th wave properties.

C. Directional wave spectra obtained from $en\eta$ data

Riedel and Healey [2] indicated that, by using the time-series combination of $en\eta$, the Fourier coefficients of the directional spreading function were determined as Equations (8) – (11). They also indicated that these coefficients were used for the Datawell Directional Waverider measuring three-component accelerations of the buoy, which were integrated to obtain three-component displacements. In this study, three-component displacements were measured directly by the GNSS buoy.

$$a_1'(f) = \frac{Im[C_{e\eta}(f)]}{\sqrt{C_{\eta\eta}(f)[C_{ee}(f)+C_{nn}(f)]}} \quad (8)$$

$$b_1'(f) = \frac{Im[C_{n\eta}(f)]}{\sqrt{C_{\eta\eta}(f)[C_{ee}(f)+C_{nn}(f)]}} \quad (9)$$

$$a_2'(f) = \frac{C_{ee}(f)-C_{nn}(f)}{C_{ee}(f)+C_{nn}(f)} \quad (10)$$

$$b_2'(f) = \frac{2Re[C_{en}(f)]}{C_{ee}(f)+C_{nn}(f)} \quad (11)$$

where Im and Re were to extract the imaginary and real part of the cross-power spectrum, respectively.

D. Directional wave spectra obtained from uvw data

Riedel and Healey [2] also indicated that by combining the uvw data measured by a tri-directional current meter, the Fourier coefficients of the directional spreading function can be determined as follows.

$$a_1'(f) = \frac{Im[C_{wu}(f)]}{\sqrt{C_{ww}(f)[C_{uu}(f)+C_{vv}(f)]}} \quad (12)$$

$$b_1'(f) = \frac{Im[C_{wv}(f)]}{\sqrt{C_{ww}(f)[C_{uu}(f)+C_{vv}(f)]}} \quad (13)$$

$$a_2'(f) = \frac{C_{uu}(f)-C_{vv}(f)}{C_{uu}(f)+C_{vv}(f)} \quad (14)$$

$$b_2'(f) = \frac{2Re[C_{uv}(f)]}{C_{uu}(f)+C_{vv}(f)} \quad (15)$$

In this study, the tri-directional current speeds were measured by the GNSS buoy.

E. The Weighted truncated Fourier series (WFS) method

By applying the WFS method proposed by Longuet-Higgins et al. [5], the above Fourier coefficients are further corrected as follows.

According to Earle [6], we found that a weighting of the Fourier coefficients could increase the width of the directional spreading function, but this approach prevented unrealistic negative values for directions far from the mean direction. The weighted truncated Fourier coefficients in Eqs. (16) – (19) were utilized to calculate the directional spreading functions. Accordingly, Eq. (3) was rewritten as Eq. (20).

$$a_1''(f) = \frac{2}{3}a_1'(f) \quad (16)$$

$$b_1''(f) = \frac{2}{3}b_1'(f) \quad (17)$$

$$a_2''(f) = \frac{1}{6}a_2'(f) \quad (18)$$

$$b_2''(f) = \frac{1}{6}b_2'(f) \quad (19)$$

$$D(f,\theta) = \frac{1}{\pi}\{\frac{1}{2} + \sum_{n=1}^{2}[a_n''(f)\cos n\theta + b_n''(f)\sin n\theta]\} \quad (20)$$

F. The mean direction and directional spreading

According to Kuik et al. [7], the mean direction ($\theta_m(f)$) and the directional spreading ($\sigma_\theta(f)$), which was a measure of the directional spreading energy, could be expressed in terms of the first-order Fourier coefficients as follows.

$$\theta_m(f) = \tan^{-1}\frac{b_1''(f)}{a_1''(f)} \quad (21)$$

$$\sigma_\theta(f) = \sqrt{2[1-(a_1''(f)\cos\theta_m(f) + b_1''(f)\sin\theta_m(f))]} \quad (22)$$

Notably, both the mean direction and the directional spreading are functions of the frequency. However, in this study, the mean direction and the directional spreading denote their values at the peak frequency.

III. Results and Discussion

A. The mean direction

The hourly time series of mean directions which are analyzed by utilizing the ηuv, $en\eta$, and uvw data of the GNSS buoy, differences in the mean directions between using $en\eta$ and ηuv, and differences in the mean directions between using uvw and ηuv are plotted in Fig. 3. The mean direction in Fig. 3 indicates the direction from which ocean waves come and the angles are measured clockwise from the north. Notably from Fig. 3 that the differences in the wave mean direction is very small; hence, the mean directions of waves are mainly identical. However, the maximum difference in the wave mean direction between the $en\eta$ and ηuv combinations is 204^o, which occurs at 00:00 October 26, 2016. The significant wave height measured by the GNSS was 0.37 m, it was quite small. The mean directions are 138^o, 342^o, and 146^o by using the ηuv, $en\eta$, and uvw combinations, respectively. The mean direction by utilizing the $en\eta$ combination is different from those of the other two combinations. Besides, according to the directional wave spectra obtained from analyzing the $en\eta$ combination during 21:00

October 25 – 02:00 October 26 (Fig. 7), the main wave is mostly coming from the south semicircle except that at 00:00 October 26. According to the rule of continuity, the directional wave spectrum, the mean direction and the dominant wave direction obtained by utilizing the $enη$ combination is abnormal at 00:00 October 26.

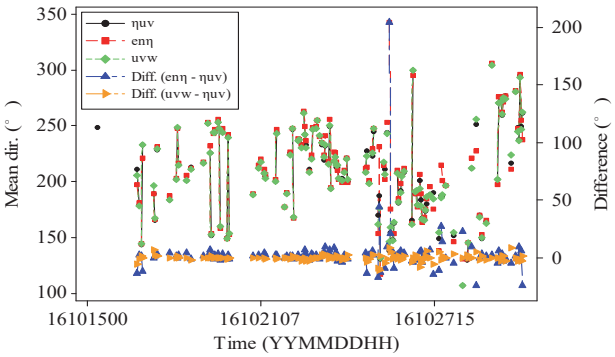

Figure 3. Hourly time-series data of mean directions and their differences

Both the mean direction and the dominant wave direction are popular-used wave directions. It's interesting to realize the difference between them. The histogram of difference between the mean direction and the dominant wave direction by using the $ηuv$ combination is plotted in Fig. 4. According to this figure, 83.8% of the difference fall into $\pm 15^o$, that is to say, mostly, two wave directions are identical. However, the maximum difference is -102^o, which occurred at 00:00 October 27. The significant wave height measured by the GNSS was 0.42 m, it was small. The shapes of histogram by using the $enη$ and uvw combinations are very similar to that obtained from the $ηuv$ combination. 82.4% and 84.8% of the difference fall into $\pm 15^o$ by using the $enη$ and uvw combinations, respectively.

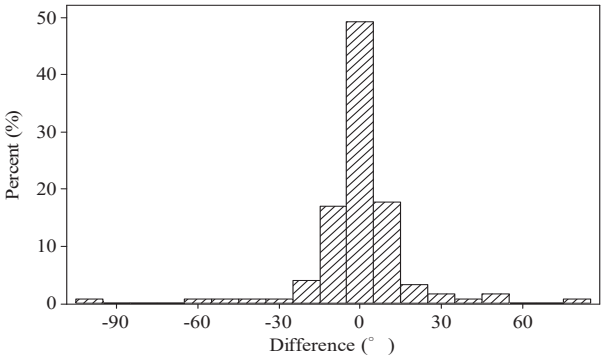

Figure 4. The histogram of difference between the mean direction and the dominant wave direction by using the $ηuv$ combination.

B. The directional spreading

The hourly time series of directional spreading obtained by using three combinations of GNSS buoy data are plotted in Fig. 5. Notably from Fig. 5 that the maximum difference between the $enη$ and $ηuv$ is 11^o and that between the uvw and $ηuv$ is 5^o. Both values are very small, indicating that the directional spreading by using three combinations is nearly identical.

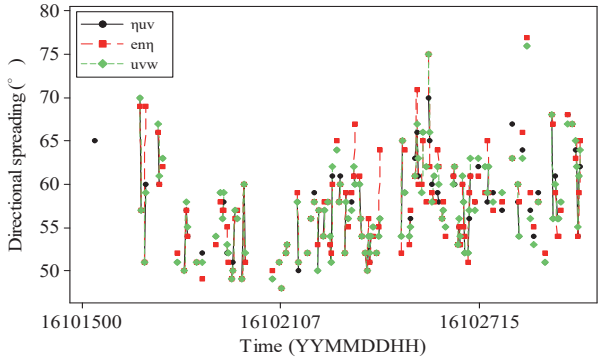

Figure 5. Hourly time series of directional spreading obtained by using various combinations of GNSS buoy data.

C. The dominant wave direction

The hourly time series of dominant wave directions and their differences obtained using three combinations of GNSS buoy data are plotted in Fig. 6. The dominant wave direction in Fig. 6 is the direction from which ocean waves come and the angles are measured clockwise from the north. We find that the differences between the uvw and $ηuv$ combinations fall into $\pm 12^o$ mostly, meanwhile, those between the $enη$ and $ηuv$ combinations fall into $\pm 30^o$ mostly (93.8%), indicating that dominant wave directions obtained by using three combinations of the GNSS buoy data are mostly identical. In Fig. 6, we find that the maximum difference in the dominant wave direction between the $enη$ and $ηuv$ combinations is 169^o. The reason is that the directional wave spectrum and the dominant wave direction are abnormal by using the $enη$ combination at 00:00 October 26, which is indicated in Section A and D.

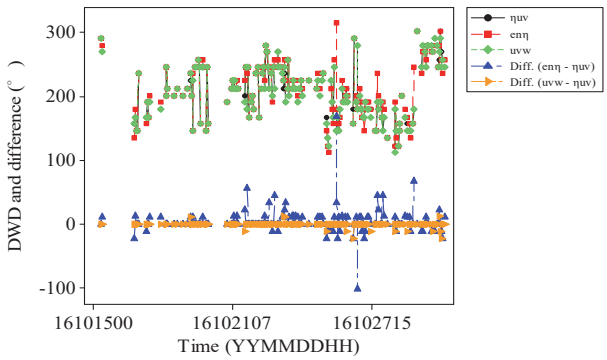

Figure 6. Hourly time series of dominant wave directions and their differences

D. The directional wave spectrum

The directional wave spectra calculated by utilizing the $enη$ (left) and $ηuv$ (right) combinations, during 21:00 October 25 - 02:00 October 26, 2016, are shown in Fig. 7. The significant wave heights measured by the GNSS were smaller than 1 m. The tangential direction of the circular plot illustrates the direction from which ocean waves come. The 0^o, 90^o, 180^o, and 270^o indicate the north, east, south, and west directions, respectively. The radial direction indicates the wave frequency in Hz. The eight-digit caption on the top indicates the year, month, day, and hour of the data, sequentially, each has two digits. Furthermore, the peak frequency and the dominant wave direction are also shown in the upper-left corner of each figure. Whenever the wind speed is larger than or equal to 1 m/s, an arrow is plotted to indicate the local wind data, on the other hand, the arrow is not shown.

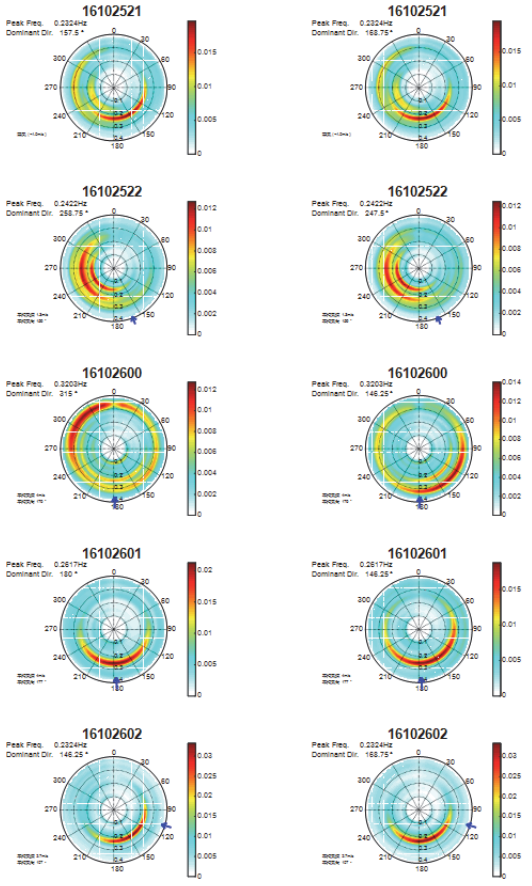

Figure 7. Directional wave spectra obtained by using the $enη$ (left) and $ηuv$ (right) combinations whenever significant wave heights are small

We find that the directional wave spectra obtained by using the $enη$ combination are similar to those by using the $ηuv$ combination, except the directional wave spectrum at 00:00 October 26. In Section A, we illustrate that the directional wave spectrum obtained by using the $enη$ combination at 00:00 October 26 is abnormal; furthermore, the peak wave energy coming from the NW direction at the frequency higher than 0.3 Hz. The dominant wave direction and the wind direction do not match. According to the dataset, among three combinations, we find that the $ηuv$ and uvw combinations are a little better for analyzing the directional wave spectrum whenever the significant wave height is small.

Fig. 8 illustrates the directional wave spectra obtained by utilizing the $ηuv$, $enη$, and uvw combinations. From 06:00 to 11:00 October 21, 2016, the significant wave heights measured by the GNSS were larger than 4.2 m. The directional wave spectra at each hour are identical. Hence, there is no difference between utilizing three time-series combinations for analyzing the directional wave spectrum whenever the significant wave heights are large. Furthermore, during the epoch of the dataset, all the peak waves come from the SW direction and the peak frequencies are very low (0.0859 Hz) because of the typhoon-induced swell. Fig. 9 shows that typhoon HAIMA is located at the WSW direction of Small Liu-qiu buoy on October 21.

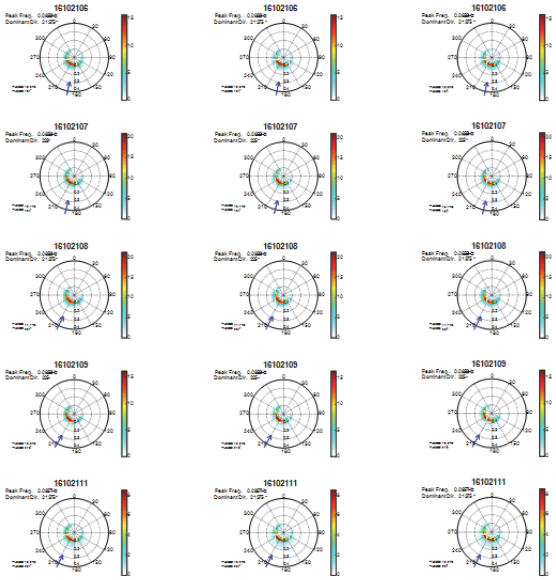

Figure 8. Directional wave spectra obtained from the $ηuv$ (left), $enη$ (middle), and uvw (right) combinations whenever significant wave heights are large

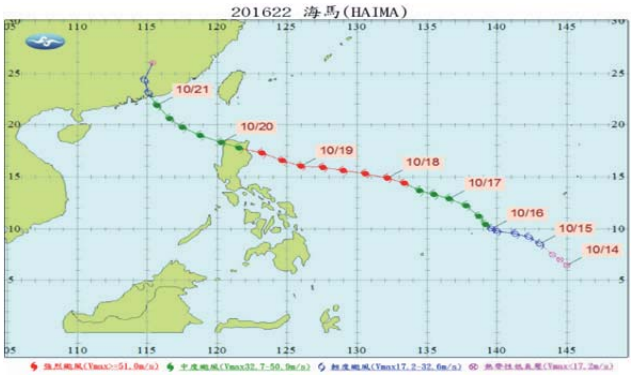

Figure 9. The path of typhoon HAIMA [8]

IV. Conclusions

Based on the WFS method, three combinations of time-series data obtained by the GNSS buoy, such as: ηuv, $en\eta$, and uvw, were used to determine the directional wave spectrum and its spectral parameters. Conclusions are itemized as follows:

1. The mean directions at the peak frequency are mostly identical by using three combinations.
2. The peak wave directions obtained by the three various combinations of the GNSS data are nearly identical.
3. The mean directions at the peak frequency and the dominant wave directions are mostly identical.
4. The directional spreading at the peak frequency is nearly identical by using three combinations.
5. The directional wave spectra are very similar by using three combinations, especially when the significant wave heights are larger than 1 m.

Acknowledgments

The authors thank the Central Weather Bureau (CWB) for providing the GNSS receiver and allowing us to integrate the GNSS receiver into the Small Liu-qiu buoy.

References

[1] Lin, Y.P., Huang, C.J., Chen, S.H., Doong, D.J., Kao, C.C., 2017. Development of A GNSS Buoy for Monitoring Water Surface Elevations in Estuaries and Coastal Areas, *Sensors*, 17, 172, doi:10.3390/s17010172.

[2] Riedel, J.S., Healey, A.J., 2005. Estimation of Directional Wave Spectra from An Autonomous Underwater Vehicle, Naval Postgraduate School, Center for Autonomous Underwater Vehicle Research, Monterey, CA, 10pp.

[3] Work, P.A., 2008. Nearshore Directional Wave Measurements by Surface-following Buoy and Acoustic Doppler Current Profiler, *Ocean Engineering,* 35(8–9), 727-737.

[4] Lin, Y.P., 2018. Development and Applications of A GNSS Buoy for Monitoring Tides and Ocean Waves in Coastal Areas, *Dissertation for Doctor of Philosophy in Hydraulic and Ocean Engineering, National Cheng Kung University, 82pp.*

[5] Longuet-Higgins, M.S., Cartwright, D.E., Smith, N.D., 1963. *Ocean Wave Spectra*, Prentice Hall, 365pp.

[6] Earle, M.D., 1996. Nondirectional and Directional Wave Data Analysis Procedures, National Data Buoy Center, National Oceanic and Atmospheric Administration, U.S. Department of Commerce, Stennis Space Center, USA, 43pp.

[7] Kuik, A.J., Van Vledder, G. PH., Holthuijsen, L.H., 1988. A Method for The Routine Analysis of Pitch-and-roll Buoy Wave Data, *Journal of Physical Oceanography,* 18(7), 1020-1034.

[8] http://rdc28.cwb.gov.tw/TDB/ntdb/pageControl/typhoon?year=2016&num=201622&name=HAIMA&from_warning=false (accessed on 29 August 2018).